Many-body approach to non-Hermitian physics in fermionic systems

Eunwoo Lee, Hyunjik Lee, and Bohm-Jung Yang

Phys. Rev. B **101**, 121109 — Published 16 March 2020

DOI: 10.1103/PhysRevB.101.121109

Many-body approach to non-Hermitian physics in fermionic systems

Eunwoo Lee,[1,2,3,*] Hyunjik Lee,[1,2,3,*] and Bohm-Jung Yang[1,2,3,†]

[1]*Department of Physics and Astronomy, Seoul National University, Seoul 08826, Korea*
[2]*Center for Correlated Electron Systems, Institute for Basic Science (IBS), Seoul 08826, Korea*
[3]*Center for Theoretical Physics (CTP), Seoul National University, Seoul 08826, Korea*
(Dated: February 27, 2020)

In previous studies, the topological invariants of 1D non-Hermitian systems have been defined in open boundary condition (OBC) to satisfy the bulk-boundary correspondence. The extreme sensitivity of bulk energy spectra to boundary conditions has been attributed to the breakdown of the conventional bulk-boundary correspondence based on the topological invariants defined under periodic boundary condition (PBC). Here we propose non-Hermitian many-body polarization as a topological invariant for 1D non-Hermitian systems defined in PBC, which satisfies the bulk-boundary correspondence. Employing many-body methodology in the non-Hermitian Su-Schrieffer-Heeger model for fermions, we show the absence of non-Hermitian skin effect due to the Pauli exclusion principle and demonstrate the bulk-boundary correspondence using the invariant defined under PBC. Moreover, we show that the bulk topological invariant is quantized in the presence of chiral or generalized inversion symmetry. Our study suggests the existence of generalized crystalline symmetries in non-Hermitian systems, which give quantized topological invariants that capture the symmetry-protected topology of non-Hermitian systems.

PACS numbers:

Introduction.— Recent progress in the study of non-Hermitian systems, such as open systems or dissipative systems with gain and loss [1–40], has uncovered various intriguing physical phenomena that do not exist in Hermitian systems. For instance, the characteristic complex energy spectra of non-Hermitian systems are theoretically predicted to host exceptional surfaces or bulk Fermi-arcs [41–58], which are later realized in experiments [59, 60]. Nowadays, there are growing research activities to extend the idea of topological Bloch theory developed in Hermitian systems to non-Hermitian Hamiltonians [61–72].

One central issue in the study of topological phenomena in non-Hermitian systems is to understand the bulk-boundary correspondence (BBC). In Hermitian systems, it is well-established that the bulk topological invariants defined by Bloch wave functions in periodic boundary condition (PBC) predict robust boundary states in systems under open boundary condition (OBC) [73–75]. Contrary to this, in non-Hermitian systems, the bulk energy spectra exhibit extreme sensitivity to boundary conditions [76–78]. For instance, in recent studies of the non-Hermitian Su-Schrieffer-Heeger (SSH) model, it was shown that the bulk eigenstates, which are extended under PBC, are exponentially localized on one-side of the finite-size system with OBC [62, 79]. This phenomenon is named the non-Hermitian skin effect in Ref. 79, which has been extensively discussed recently [79–89]. Since the energy spectra under PBC and OBC differ so drastically, there has been even a common belief that the bulk invariant defined under PBC has intrinsic limitations in explaining BBC of non-Hermitian systems in general. To circumvent this problem, several interesting theoretical ideas are proposed under OBC, such as generalized Bloch theory [61–64], transfer matrix approach [65], and entanglement spectrum analysis [66]. Lack of proper topological invariants defined under PBC that satisfy BBC gives the impression that the BBC of non-Hermitian systems belongs to a rather special category which is distinct from that of Hermitian systems. However, is it really true that the BBC of non-Hermitian topological systems evades the theoretical framework developed to understand the topological phases in Hermitian systems?

Here we address this important question focusing on 1D fermionic non-Hermitian systems. For the non-Hermitian SSH model describing spinless fermions, we show that the non-Hermitian skin effect, observed in a single-particle approach, does not appear in the many-body approach due to the Pauli exclusion principle [90]. We have also found that at half-filling, topologically trivial and non-trivial phases display the same charge density distribution in systems with OBC. When one extra electron or hole is added, however, the additional charge is exponentially localized near the edges when the system is topologically non-trivial, whereas it spreads over the entire system when the system is topologically trivial.

Moreover, we have identified a bulk topological invariant defined under PBC: the non-Hermitian many-body polarization, which correctly describes the BBC and gives the same bulk critical points for topological phase transitions as those predicted under OBC [79]. We find that the many-body polarization defined under PBC is quantized in the presence of chiral or generalized inversion symmetry. This clearly shows that, in non-Hermitian systems, one can define bulk topological invariants under PBC, which are quantized due to generalized crystalline symmetries and correctly predict the associated boundary states, as in the case of conventional fermionic Hermitian systems. Finally, we propose the non-Hermitian version of the edge entanglement entropy that can be used to detect the edge degeneracy in 1D non-Hermitian systems.

Model.— The non-Hermitian SSH model Hamiltonian $\hat{H}_{\rm SSH}$ is composed of two parts as $\hat{H}_{\rm SSH} = \hat{H}_0 + \hat{H}_{\rm NH}$ in

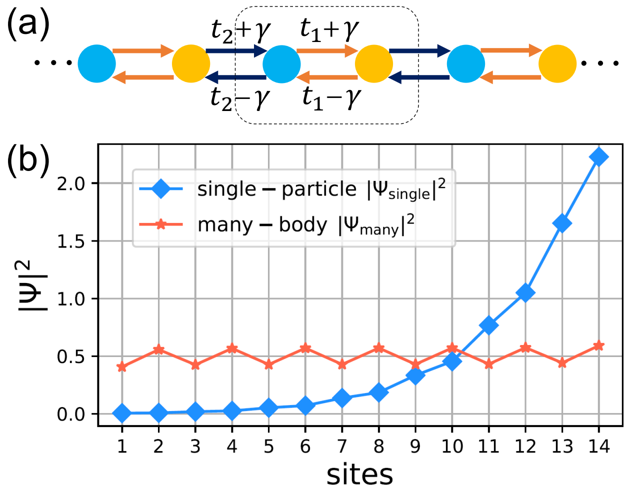

FIG. 1: (Color Online) (a) Schematic figure describing the non-Hermitian SSH model for spinless fermions. The dotted box denotes the unit cell. t_1 (t_2) indicates the intracell (intercell) hopping while γ denotes the asymmetric hopping term that makes the system to be non-Hermitian. (b) Distribution of the particle density $|\Psi(i)|^2$ from single-particle wave functions (square dots) and many-body wave functions (star-shaped dots) obtained by solving a finite-size chain with 14 sites under OBC. We choose the model parameters $t_1 = 2, t_2 = 1, \gamma = 0.3$ which correspond to a trivial insulator. To obtain $|\Psi(i)|^2$ from single-particle wave functions, the contributions from all states below the gap are added.

which

$$\hat{H}_0 = \sum_i \left\{ \left[J - \Delta J(-1)^i\right] \hat{c}_i^\dagger \hat{c}_{i+1} + h.c.\right\}, \quad (1)$$

$$\hat{H}_{\rm NH} = \sum_i \gamma(\hat{c}_{i+1}^\dagger \hat{c}_i - \hat{c}_i^\dagger \hat{c}_{i+1}), \quad (2)$$

where $\hat{c}_i$ ($\hat{c}_i^\dagger$) denotes the electron annihilation (creation) operator at the i-th site. $\hat{H}_0$ indicates the Hermitian SSH Hamiltonian with the intracell (intercell) hopping amplitude $t_1 = J+\Delta J$ ($t_2 = J-\Delta J$) while $\hat{H}_{\rm NH}$ denotes the non-Hermitian part describing asymmetric hopping processes. [See Fig. 1 (a).] The model is equivalent to Creutz-ladder-like system with gain and loss, which is experimentally realizable in ultracold fermionic system [62, 91].

Diagonalizing the Hamiltonian $\hat{H}_{\rm SSH}$ under OBC and using the corresponding single-particle eigenvector $|\psi_n\rangle$ with the band index n, one can obtain the particle density at the i-th site $|\Psi_{\rm single}(i)|^2 \equiv \sum_{n\in {\rm occ}} \langle\psi_n|\hat{c}_i^\dagger \hat{c}_i|\psi_n\rangle$. Here we have added the contribution from all the single-particle wave functions below the Fermi level, as plotted in Fig. 1 (b) with square dots. One can observe the exponential localization of the particle density on the right edge, manifesting the non-Hermitian skin effect. However, this accumulation obviously violates the Pauli exclusion principle, which should be corrected to obtain physically meaningful results [90].

To take into account of Fermi statistics, we take the many-body approach using Fock basis states. For a system with L lattice sites filled with N electrons, the number of allowed Fock basis states is given by $\binom{L}{N}$. For example, a 4-site system filled with 2 electrons has 6 Fock basis states: $|1100\rangle, |1010\rangle, |1001\rangle, |0110\rangle, |0101\rangle, |0011\rangle$ where 0 and 1 indicate the number of electron at each site. The Hamiltonian acts on Fock bases as follows: $\hat{c}_3^\dagger \hat{c}_2|1100\rangle = |1010\rangle$, $\hat{c}_3^\dagger \hat{c}_2|0110\rangle = 0$, and so on. Since a single-particle Hamiltonian is of the form $\hat{H} = \sum_{i,j} {\rm H}_{ij}\hat{c}_i^\dagger \hat{c}_j$ where ${\rm H}_{ij}$ denotes its (i,j)-th element, the (α,β)-th element of the Hamiltonian in Fock space ${\rm H^F}_{\alpha\beta}$ can be obtained as ${\rm H^F}_{\alpha\beta} = \pm{\rm H}_{ij}$ when $\langle\alpha|\hat{c}_i^\dagger \hat{c}_j|\beta\rangle = \pm 1$ for Fock bases $|\alpha\rangle, |\beta\rangle$, while ${\rm H^F}_{\alpha\beta} = 0$ otherwise. ${\rm H^F}$ is diagonalized using the exact diagonalization method.

In Fig. 1 (b), we plot the particle density distribution $|\Psi_{\rm many}(i)|^2 \equiv \langle\Psi_R^G|\hat{c}_i^\dagger \hat{c}_i|\Psi_R^G\rangle$ with star-shaped dots, where $|\Psi_R^G\rangle$ is the many-body ground state wave function that satisfies ${\rm H^F}|\Psi_R^G\rangle = E|\Psi_R^G\rangle$. The sum of the wavefunction density is normalized to N, which is the total particle number of the system. One can observe only mild slanting of particle densities instead of the exponential localization [91]. The absence of non-Hermitian skin effect in fermionic systems prompts a question: what happens to BBC when many-body formalism is used?

Biorthogonal formulation.— To describe the topological property of the many-body wave functions, we adopt the formulation of biorthogonal quantum mechanics. In general, a diagonalizable non-Hermitian matrix H can have different left and right eigenvectors $|\Psi_L\rangle, |\Psi_R\rangle$ that satisfy [55]

$$ {\rm H}|\Psi_{R,n}\rangle = E_n|\Psi_{R,n}\rangle, \;\; {\rm H}^\dagger|\Psi_{L,n}\rangle = E_n^*|\Psi_{L,n}\rangle. \quad (3)$$

The sets of eigenvectors can be chosen to satisfy the biorthonormality condition $\langle\Psi_{L,n}|\Psi_{R,m}\rangle = \delta_{nm}$, which ensures that the transition amplitude $|\langle\Psi_{L,n}|\Psi_{R,m}\rangle|^2$ between two states with different energy eigenvalues is zero. In this paper, we focus on the Hamiltonian matrices with biorthogonality.

The biorthogonal bases naturally construct the identity operator as $\hat{\mathbb{1}} = \sum_n |\Psi_{R,n}\rangle\langle\Psi_{L,n}|$. The expectation value of the observable in a pure right state $|\Psi_R\rangle = \sum_n C_n|\Psi_{R,n}\rangle$ is expressed as

$$\langle\hat{O}\rangle = \langle\Psi_L|\hat{O}|\Psi_R\rangle, \quad (4)$$

where $|\Psi_L\rangle = \sum_n C_n|\Psi_{L,n}\rangle$, such that $\langle\Psi_L|\Psi_R\rangle = \sum_n C_n^* C_n = 1$. The corresponding particle density at the site i is given by $|\Psi_{LR}(i)|^2 \equiv \langle\Psi_L|\hat{c}_i^\dagger \hat{c}_i|\Psi_R\rangle$. Let us note that $|\Psi_{LR}(i)|^2$ is different from the conventional particle density, which is relevant to $|\Psi_{RR}(i)|^2 \equiv \langle\Psi_R|\hat{c}_i^\dagger \hat{c}_i|\Psi_R\rangle/\langle\Psi_R|\Psi_R\rangle$ in terms of biorthogonal formulation.

Topological zero-modes.— One of the most prominent characteristics of the SSH model that distinguishes the topologically trivial and non-trivial phases is the existence of zero-modes at the edge. To confirm the existence of the zero-modes in the non-Hermitian SSH model, $|\Psi_{LR}(i)|^2$ is computed by using the ground state many-body wave function

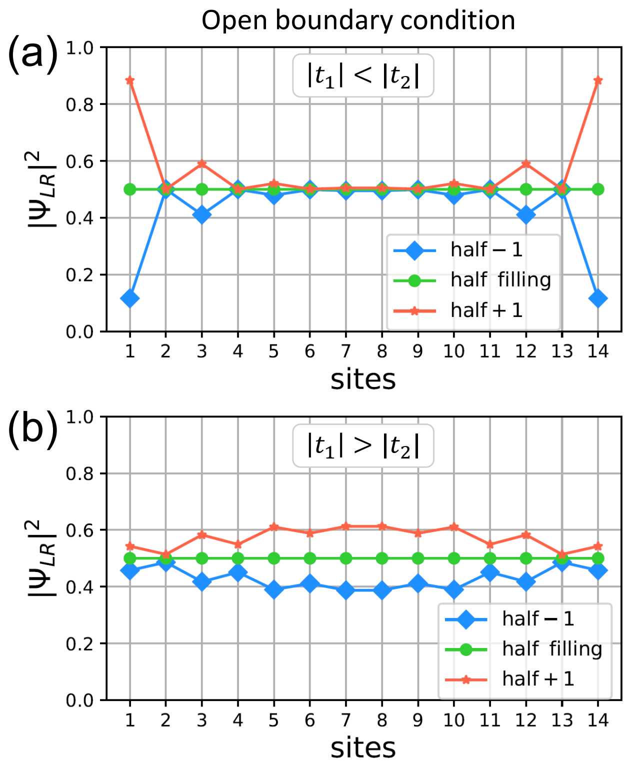

FIG. 2: (Color Online) Distribution of $|\Psi_{LR}(i)|^2$ for a non-Hermitian SSH chain with 14 sites under OBC. (a) Topological insulator where $t_1 = 1,\ t_2 = 2,\ \gamma = 0.3$. At half-filling, $|\Psi_{LR}|^2$ is uniformly distributed. Adding (subtracting) an electron, the extra electron density is accumulated (depleted) at the edges, which shows the existence of topological zero modes localized at the edges. The zero-mode is always observed when $|t_1| < |t_2|$. (b) Trivial insulator where $t_1 = 2,\ t_2 = 1,\ \gamma = 0.3$. At half-filling, the electron density is uniformly distributed as in the case of the topological insulator. Adding (subtracting) an electron, the extra electron density accumulated (depleted) spreads throughout the bulk, showing the absence of localized zero-modes.

$\{|\Psi_L^G\rangle, |\Psi_R^G\rangle\}$ as shown in Fig. 2. At half-filling, the distribution of $|\Psi_{LR}(i)|^2$ is uniform in both trivial and topological phases. However, when one electron or hole is added, the extra charge is localized at the edges in topological phases. In contrast, in trivial phases, the extra charge is spread over the entire system. The localized edge modes are always present (absent) when $|t_1| < |t_2|$ ($|t_1| > |t_2|$) [91]. Moreover, when $|t_1| < |t_2|$, the ground state energy does not change when one electron is added or subtracted. This means that the states localized at the edges are indeed zero-energy edge modes. When $|t_2| < |t_1|$, on the other hand, adding (subtracting) an electron increases (decreases) the energy as much as the energy gap. Namely, the topological phase transition between the trivial and topological insulators occurs at $|t_2| = |t_1|$. The location of the critical point is the same as that from the generalized Brillouin zone approach under OBC [79]. Note that the entire energy spectrum of our model is real in OBC when $|\gamma| < |t_1|, |t_2|$ [91].

Let us now obtain the critical points obtained under PBC. Naive application of the Bloch theory in PBC predicts the closing of bulk gaps at $t_2 = t_1 \pm 2\gamma$ or $t_2 = -t_1$, which is not consistent with the critical point where the zero-modes appear or disappear [92]. Such a discrepancy occurs because the energy eigenvalues obtained in PBC are not real, but generally complex. Interestingly, in our model, the many-body ground state energy of H^{F} in PBC is real and thus physically stable when $|\gamma| < |t_1|, |t_2|$ and $N = L/2$ is an odd integer [91]. The distribution of the particle density of the system in PBC is shown in Fig. 3(a) obtained by using the many-body ground state.

Non-Hermitian polarization.— In order to discuss the topological phase in PBC, we need to define a bulk topological invariant. In Hermitian systems, the many-body bulk polarization is a well-defined 1D topological invariant, whose definition under PBC is given by [93]

$$P \equiv \lim_{N\to\infty} \frac{1}{2\pi} \mathrm{Im} \ln \langle \Psi^G | e^{i\frac{2\pi}{N}\hat{X}} | \Psi^G \rangle \mod 1, \tag{5}$$

where $|\Psi^G\rangle$ is the many-body ground state and N is the number of unit-cells. Here $\hat{X}$ denotes the summation of position operators for all atoms. P is quantized in the presence of either inversion or chiral symmetry. The Hamiltonian $\hat{H}$ invariant under the chiral $\hat{S}$ or inversion $\hat{I}$ symmetry satisfies

$$\hat{S}\hat{H}\hat{S}^{-1} = \hat{H},\ \ \hat{I}\hat{H}\hat{I}^{-1} = \hat{H}, \tag{6}$$

where $\hat{S}\hat{c}_i\hat{S}^{-1} = (-1)^i \hat{c}_i^\dagger$, $\hat{S}i\hat{S} = -i$ and $\hat{I}\hat{c}_i\hat{I}^{-1} = \hat{c}_{L+1-i}$, $\hat{I}i\hat{I}^{-1} = i$ [94]. In terms of the corresponding matrix representation S and I, the invariance of the Hamiltonian matrix H becomes

$$S^{-1}\mathrm{H}S = -\mathrm{H},\ \ I^{-1}\mathrm{H}I = \mathrm{H}. \tag{7}$$

Under inversion symmetry, the polarization satisfies $P \equiv -P \mod 1$, so that it is quantized into either 0 or $1/2 \mod 1$. Also, chiral symmetry imposes $P_{\text{occ}} = P_{\text{unocc}}$ with $P_{\text{occ}} + P_{\text{unocc}} = 0 \mod 1$, which lead to the polarization quantization: $P_{\text{occ}} = 0$ or $1/2 \mod 1$. Here P_{occ} (P_{unocc}) denotes the polarization of occupied (unoccupied) states.

We extend the idea of the many-body bulk polarization, which has been used in Hermitian systems only, to non-Hermitian systems by defining the non-Hermitian many-body bulk polarization P^{LR} as

$$P^{LR} \equiv \lim_{N\to\infty} \frac{1}{2\pi} \mathrm{Im} \ln \langle \Psi_L^G | e^{i\frac{2\pi}{N}\hat{X}} | \Psi_R^G \rangle \mod 1, \tag{8}$$

where $|\Psi_R^G\rangle$ ($|\Psi_L^G\rangle$) is the right (left) many-body ground state. Here, we introduce chiral and generalized inversion symmetries for non-Hermitian systems, which quantize P^{LR}, as follows

$$\hat{S}\hat{H}\hat{S}^{-1} = \hat{H}^\dagger,\ \ \hat{I}\hat{H}\hat{I}^{-1} = \hat{H}^\dagger. \tag{9}$$

In terms of the corresponding matrix representation, we have

$$S^{-1}\mathrm{H}S = -\mathrm{H},\ \ I^{-1}\mathrm{H}I = \mathrm{H}^\dagger. \tag{10}$$

Note that $\hat{H}_{\text{SSH}}$ has both chiral and generalized inversion symmetry. One can also check the existence of these symmetries in Fock space representation as well. Under generalized inversion symmetry, $P^{LR} \equiv -P^{LR} \mod 1$, and thus P^{LR} is quantized into 0 or $1/2$. Likewise, under chiral symmetry, $P^{LR}_{\text{occ}} = P^{LR}_{\text{unocc}}$ results in the quantization of P^{LR}_{occ} with the condition $P^{LR}_{\text{occ}} + P^{LR}_{\text{unocc}} = 0 \mod 1$ [91]. Therefore in the presence of either chiral or generalized inversion symmetry, the non-Hermitian many-body polarization is quantized into either 0 or $1/2$.

As shown in Fig. 3 (b), P^{LR} defined under PBC is $1/2$ when $|t_1| < |t_2|$ whereas it is 0 when $|t_1| > |t_2|$. The phase transition occurs at the critical point $|t_1| = |t_2|$, which is consistent with the numerical study of the zero-modes in OBC discussed before. In fact, one can understand the reason why the critical point is located at $|t_1| = |t_2|$ as follows. Switching the role of t_1 and t_2 is equivalent to translating the system by a half lattice constant. Then ith site moves to the $(i+1)$th site. Thus, P^{LR} with $t_1 = \alpha, t_2 = \beta$ is different by $1/2$ from P^{LR} with $t_1 = \beta, t_2 = \alpha$ [91]. The location of the critical point agrees with the numerical and analytical results obtained under OBC [91] indicating that BBC is satisfied when P^{LR} defined under PBC is considered. This is also confirmed in another model as well [91].

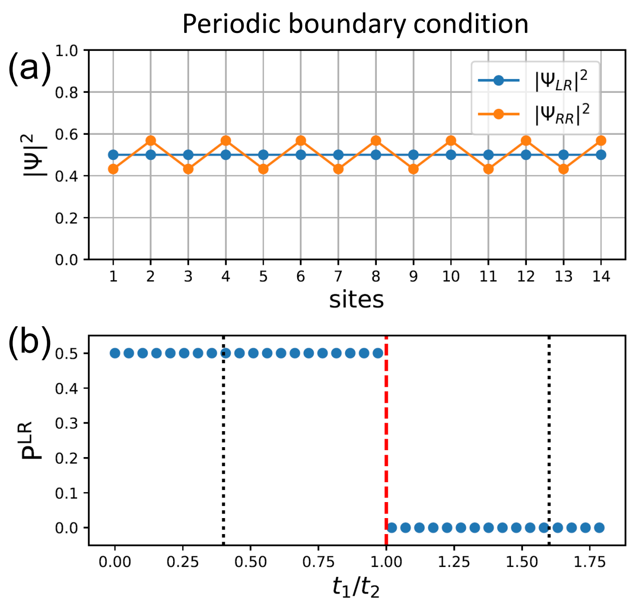

FIG. 3: (Color Online) (a) Distribution of the particle densities $|\Psi_{LR}(i)|^2$ and $|\Psi_{RR}(i)|^2$ at half-filling, for a non-Hermitian SSH model with 14 sites under PBC. We use the model parameters $t_1 = 2$, $t_2 = 1$, $\gamma = 0.3$ that corresponds to a trivial phase. $|\Psi_{LR}|^2$ is uniform whereas $|\Psi_{RR}|^2$ has a saw-tooth shape. (b) Non-Hermitian many-body polarization P^{LR} as a function of t_1 with $t_2 = 1$, $\gamma = 0.3$. When $0 < t_1 < t_2$ ($t_1 > t_2 > 0$), $P^{LR} = 1/2$ ($P^{LR} = 0$). The critical point $t_1 = t_2$ is consistent with the numerical study of the zero-modes under OBC. Thus, the BBC can be described by using P^{LR}. The black dotted vertical lines indicate the locations of gap-closing points obtained by Bloch Hamiltonian, which cannot explain the BBC.

Edge entanglement entropy.— Another way to determine the topological property of many-body systems is to calculate the edge entanglement entropy, which is known to be useful in detecting the edge degeneracy [73, 95–97]. In particular, when there are two zero-modes localized at the edges of a 1D topological isulator, edge entanglement entropy is quantized to $\ln 2$ [95].

To define the entanglement entropy, we consider a system that is divided into two subsystems A and B. In Hermitian systems, the Rényi entropy S_α of order α is defined as

$$S_\alpha = \frac{1}{1-\alpha} \ln \mathrm{Tr}[(\rho_A)^\alpha], \tag{11}$$

where ρ_A is the reduced density matrix for the subsystem A and $\alpha \geq 0, \alpha \neq 1$. Similar to the way of defining non-Hermitian many-body polarization, we introduce Rényi entropy S_α for non-Hermitian systems as

$$S^{LR}_\alpha \equiv \frac{1}{1-\alpha} \ln \mathrm{Tr}[(\rho^{RL}_A)^\alpha], \tag{12}$$

where $\rho^{RL} = |\Psi_R\rangle\langle\Psi_L|$.

The edge entanglement entropy $S^{LR}_{\alpha,\text{edge}}$ is defined as

$$S^{LR}_{\alpha,\text{edge}} \equiv S^{LR}_{\alpha,\text{OBC}} - \frac{1}{2} S^{LR}_{\alpha,\text{PBC}}, \tag{13}$$

where $S^{LR}_{\alpha,\text{OBC}}(S^{LR}_{\alpha,\text{PBC}})$ is calculated under OBC (PBC). Since the entanglement entropy follows the area law, the leading term of the entanglement entropy $S^{LR}_{\alpha,\text{PBC}}$ is about twice larger than that of $S^{LR}_{\alpha,\text{OBC}}$. Thus, $\frac{1}{2}S^{LR}_{\alpha,\text{PBC}}$ is subtracted to cancel out the leading terms, and what remains in $S^{LR}_{\alpha,\text{edge}}$ is the subleading term that detects degenerate edge states in OBC that is quantized to 0 or $\ln 2$ in thermodynamic limit.

As shown in Fig. 4(a), $S^{LR}_{2,\text{edge}}$ is ln2 for a topological phase and 0 for a trivial phase, where we choose $\alpha = 2$ for the convenience of calculation. Meanwhile, if we utilize the conventional entanglement entropy $S_{2,\text{edge}} = S_{2,\text{OBC}} - \frac{1}{2}S_{2,\text{PBC}}$, the entropy plummets as the asymmetric hopping amplitude increases [See Fig. 4(b)]. Thus, the topological propertiy of the non-Hermitian system cannot be correctly captured unless we use the biorthogonal formalism.

Discussion.— Our theoretical approach based on many-body wave functions suggests that careful consideration of Fermi statistics leads to the recovery of the conventional BBC even in non-Hermitian systems. Since the non-Hermitian skin effect has been observed in various non-Hermitian Hamiltonians in different dimensions, and the resulting exponential accumulation of charge densities always violates the Pauli exclusion principle, we believe that our theoretical results are valid in general non-Hermitian fermionic systems. Extending the many-body approach to higher dimensional non-Hermitian systems is definitely one important direction for future research.

Moreover, the identification of the non-Hermitian many-body polarization that is quantized under generalized inversion symmetry clearly shows the interplay between the crystalline symmetries and non-Hermitian topology. This indicates the existence of symmetry-protected topological phases

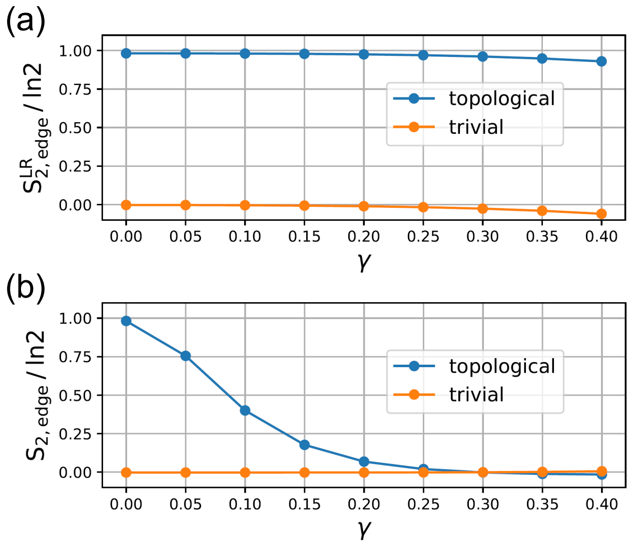

FIG. 4: (Color Online) (a) Non-Hermitian edge entanglement entropy $S^{LR}_{2,\text{edge}}$ which detects edge degeneracy at two edges. A finite-size non-Hermitian SSH chain with 14 sites is considered. $S^{LR}_{2,\text{edge}} = \ln 2$ if the ground state is topological whereas $S^{LR}_{2,\text{edge}} = 0$ if the ground-state is trivial. The deviation from the quantized values at large γ is due to the finite-size effect, which becomes smaller as the length of the system increases. (b) The conventional edge entanglement entropy calculated using only right eigenstates. The entropy of the trivial phase is consistently zero, whereas the topological phase's entropy plummets as the asymmetric hopping amplitude increases.

even in non-Hermitian systems. We believe that this discovery will open a new avenue to search topological non-Hermitian systems protected by crystalline symmetries. Finally, since the topological invariant is defined by using many-body formulation, our work can be easily extended to interacting non-Hermitian systems as well.

Acknowledgement.— We thank Seunghun Lee, Yoonseok Hwang, and Junyeong Ahn for useful discussions. E. L., H. L., and B.-J.Y. were supported by the Institute for Basic Science in Korea (Grant No. IBS-R009-D1) and Basic Science Research Program through the National Research Foundation of Korea (NRF) (Grant No. 0426-20190008), and the POSCO Science Fellowship of POSCO TJ Park Foundation (No. 0426-20180002). This work was supported in part by the U.S. Army Research Office under Grant Number W911NF-18-1-0137.

---

* equal contribution
† Electronic address: bjyang@snu.ac.kr

[1] M. Znojil, arXiv preprint math-ph/0104012 (2001).
[2] C. M. Bender, Contemporary physics **46**, 277 (2005).
[3] C. M. Bender, Reports on Progress in Physics **70**, 947 (2007).
[4] I. Rotter, Journal of Physics A: Mathematical and Theoretical **42**, 153001 (2009).
[5] H.J. Carmichael, Physical review letters **70**, 2273 (1993).
[6] S. Diehl, E. Rico, M. A. Baranov, and P. Zoller, Nature Physics **7**, 971 (2011).
[7] S. Malzard, C. Poli, and H. Schomerus, Physical review letters **115**, 200402 (2015).
[8] T. E. Lee and C.-K. Chan, Physical Review X **4**, 041001 (2014).
[9] T. E. Lee, F. Reiter, and N. Moiseyev, Physical review letters **113**, 250401 (2014).
[10] K. G. Makris, R. El-Ganainy, D. N. Christodoulides, and Z. H. Musslimani, Physical Review Letters **100**, 103904 (2008).
[11] S. Klaiman, U. Günther, and N. Moiseyev, Physical review letters **101**, 080402 (2008).
[12] A. Regensburger, C. Bersch, M.-A. Miri, G. Onishchukov, D. N. Christodoulides, and U. Peschel, Nature **488**, 167 (2012).
[13] C. E. Rüter, K. G. Makris, R. El-Ganainy, D. N. Christodoulides, M. Segev, and D. Kip, Nature physics **6**, 192 (2010).
[14] Z. Lin, H. Ramezani, T. Eichelkraut, T. Kottos, H. Cao, and D. N. Christodoulides, Physical Review Letters **106**, 213901 (2011).
[15] L. Feng, Y.-L. Xu, W. S. Fegadolli, M.-H. Lu, J. E. Oliveira, V. R. Almeida, Y.-F. Chen, and A. Scherer, Nature materials **12**, 108 (2013).
[16] A. Guo, G.J. Salamo, D. Duchesne, R. Morandotti, M. Volatier-Ravat, V. Aimez, G. A. Siviloglou, and D. N. Christodoulides, Physical Review Letters **103**, 093902 (2009).
[17] M. Liertzer, L. Ge, A. Cerjan, A. D. Stone, H. E. Türeci, and S. Rotter, Physical Review Letters **108**, 173901 (2012).
[18] B. Peng, Ş. Özdemir, S. Rotter, H. Yilmaz, M. Liertzer, F. Monifi, C. Bender, F. Nori, and L. Yang, Science **346**, 328 (2014).
[19] R. Fleury, D. Sounas, and A. Alu, Nature communications **6**, 5905 (2015).
[20] L. Chang, X. Jiang, S. Hua, C. Yang, J. Wen, L. Jiang, G. Li, G. Wang, and M. Xiao, Nature photonics **8**, 524 (2014).
[21] H. Hodaei, A. U. Hassan, S. Wittek, H. Garcia-Gracia, R. El-Ganainy, D. N. Christodoulides, and M. Khajavikhan, Nature **548**, 187 (2017).
[22] H. Hodaei, M.-A. Miri, M. Heinrich, D. N. Christodoulides, and M. Khajavikhan, Science **346**, 975 (2014).
[23] L. Feng, Z. J. Wong, R.-M. Ma, Y. Wang, and X. Zhang, Science **346**, 972 (2014).
[24] T. Gao, E. Estrecho, K. Bliokh, T. Liew, M. Fraser, S. Brodbeck, M. Kamp, C. Schneider, S. Höfling, Y. Yamamoto, et al., Nature **526**, 554 (2015).
[25] H. Xu, D. Mason, L. Jiang, and J. Harris, Nature **537**, 80 (2016).
[26] Y. Ashida, S. Furukawa, and M. Ueda, Nature communications **8**, 15791 (2017).
[27] K. Kawabata, Y. Ashida, and M. Ueda, Physical review letters **119**, 190401 (2017).
[28] W. Chen, Ş. K. Özdemir, G. Zhao, J. Wiersig, and L. Yang, Nature **548**, 192 (2017).
[29] K. Ding, G. Ma, M. Xiao, Z. Q. Zhang, and C. T. Chan, Physical Review X **6**, 021007 (2016).
[30] C. A. Downing and G. Weick, Physical Review B **95**, 125426 (2017).
[31] T. Ozawa, H. M. Price, A. Amo, N. Goldman, M. Hafezi, L. Lu, M. C. Rechtsman, D. Schuster, J. Simon, O. Zilberberg, et al., Reviews of Modern Physics **91**, 015006 (2019).
[32] L. Lu, J. D. Joannopoulos, and M. Soljačić, Nature photonics **8**, 821 (2014).
[33] R. El-Ganainy, K. G. Makris, M. Khajavikhan, Z. H. Musslimani, S. Rotter, and D. N. Christodoulides, Nature Physics **14**, 11 (2018).
[34] S. Longhi, EPL (Europhysics Letters) **120**, 64001 (2018).

[35] V. V. Konotop, J. Yang, and D. A. Zezyulin, Reviews of Modern Physics **88**, 035002 (2016).
[36] H. Cao and J. Wiersig, Reviews of Modern Physics **87**, 61 (2015).
[37] J. Doppler, A. A. Mailybaev, J. Böhm, U. Kuhl, A. Girschik, F. Libisch, T. J. Milburn, P. Rabl, N. Moiseyev, and S. Rotter, Nature **537**, 76 (2016).
[38] S. Lapp, F. A. An, B. Gadway, et al., New Journal of Physics **21**, 045006 (2019).
[39] J. Y. Lee, J. Ahn, H. Zhou, and A. Vishwanath, arXiv preprint arXiv:1906.08782 (2019).
[40] Y. Ashida and M. Ueda, Physical review letters **120**, 185301 (2018).
[41] Z. Yang and J. Hu, Physical Review B **99**, 081102(R) (2019).
[42] T. Yoshida, R. Peters, N. Kawakami, and Y. Hatsugai, Physical Review B **99**, 121101(R) (2019).
[43] J. C. Budich, J. Carlström, F. K. Kunst, and E. J. Bergholtz, Physical Review B **99**, 041406(R) (2019).
[44] R. Okugawa and T. Yokoyama, Physical Review B **99**, 041202(R) (2019).
[45] K. Moors, A. A. Zyuzin, A. Y. Zyuzin, R. P. Tiwari, and T. L. Schmidt, Physical Review B **99**, 041116(R) (2019).
[46] J. Carlström and E. J. Bergholtz, Physical Review A **98**, 042114 (2018).
[47] H. Zhou, J. Y. Lee, S. Liu, and B. Zhen, Optica **6**, 190 (2019).
[48] W. Heiss, Journal of Physics A: Mathematical and Theoretical **45**, 444016 (2012).
[49] J. Carlström, M. Stålhammar, J. C. Budich, and E. J. Bergholtz, Physical Review B **99**, 161115(R) (2019).
[50] B. Midya, H. Zhao, and L. Feng, Nature communications **9**, 2674 (2018).
[51] V. Kozii and L. Fu, arXiv preprint arXiv:1708.05841 (2017).
[52] A. Mostafazadeh, Journal of Mathematical Physics **43**, 205 (2002).
[53] A. Mostafazadeh, Journal of Mathematical Physics **43**, 2814 (2002).
[54] A. Mostafazadeh, Journal of Mathematical Physics **43**, 3944 (2002).
[55] D. C. Brody, Journal of Physics A: Mathematical and Theoretical **47**, 035305 (2013).
[56] C. H. Lee, G. Li, Y. Liu, T. Tai, R. Thomale, and X. Zhang, arXiv preprint arXiv:1812.02011 (2018).
[57] L. Li, C. H. Lee, and J. Gong, Physical Review B **100**, 075403 (2019).
[58] T. Yoshida, R. Peters, and N. Kawakami, Physical Review B **98**, 035141 (2018).
[59] H. Zhou, C. Peng, Y. Yoon, C. W. Hsu, K. A. Nelson, L. Fu, J. D. Joannopoulos, M. Soljačić, and B. Zhen, Science **359**, 1009 (2018).
[60] K. Ding, G. Ma, Z. Q. Zhang, and C. T. Chan, Physical review letters **121**, 085702 (2018).
[61] F. Song, S. Yao, and Z. Wang, arXiv preprint arXiv:1905.02211 (2019).
[62] K. Yokomizo and S. Murakami, Physical review letters **123**, 066404 (2019).
[63] T.-S. Deng and W. Yi, arXiv preprint arXiv:1903.03811 (2019).
[64] S. Yao, F. Song, and Z. Wang, Physical review letters **121**, 136802 (2018).
[65] F. K. Kunst and V. Dwivedi, Physical Review B **99**, 245116 (2019).
[66] L. Herviou, N. Regnault, and J. H. Bardarson, arXiv preprint arXiv:1908.09852 (2019).
[67] E. Edvardsson, F. K. Kunst, and E. J. Bergholtz, Physical Review B **99**, 081302(R) (2019).
[68] H.-G. Zirnstein, G. Refael, and B. Rosenow, arXiv preprint arXiv:1901.11241 (2019).
[69] K.-I. Imura and Y. Takane, Physical Review B **100**, 165430 (2019).
[70] H. Wu, L. Jin, and Z. Song, arXiv preprint arXiv:1905.11576 (2019).
[71] T. Yoshida, K. Kudo, and Y. Hatsugai, Scientific reports **9**, 1 (2019).
[72] Z. Gong, Y. Ashida, K. Kawabata, K. Takasan, S. Higashikawa, and M. Ueda, Physical Review X **8**, 031079 (2018).
[73] S. Ryu and Y. Hatsugai, Physical review B **73**, 245115 (2006).
[74] F. Grusdt, M. Höning, and M. Fleischhauer, Physical review letters **110**, 260405 (2013).
[75] J.-W. Rhim, J. Behrends, and J. H. Bardarson, Physical Review B **95**, 035421 (2017).
[76] F. K. Kunst, E. Edvardsson, J. C. Budich, and E. J. Bergholtz, Physical review letters **121**, 026808 (2018).
[77] Y. Xiong, Journal of Physics Communications **2**, 035043 (2018).
[78] L. Jin and Z. Song, Physical Review B **99**, 081103(R) (2019).
[79] S. Yao and Z. Wang, Physical review letters **121**, 086803 (2018).
[80] F. Song, S. Yao, and Z. Wang, arXiv preprint arXiv:1904.08432 (2019).
[81] S. Longhi, Physical Review Research **1**, 023013 (2019).
[82] V. M. Alvarez, J. B. Vargas, M. Berdakin, and L. F. Torres, The European Physical Journal Special Topics **227**, 1295 (2018).
[83] C. H. Lee and R. Thomale, Physical Review B **99**, 201103(R) (2019).
[84] D. S. Borgnia, A. J. Kruchkov, and R.-J. Slager, arXiv preprint arXiv:1902.07217 (2019).
[85] K. Zhang, Z. Yang, and C. Fang, arXiv preprint arXiv:1910.01131 (2019).
[86] N. Okuma, K. Kawabata, K. Shiozaki, and M. Sato, arXiv preprint arXiv:1910.02878 (2019).
[87] T. Hofmann, T. Helbig, F. Schindler, N. Salgo, M. Brzezińska, M. Greiter, T. Kiessling, D. Wolf, A. Vollhardt, A. Kabaši, et al., arXiv preprint arXiv:1908.02759 (2019).
[88] T. Helbig, T. Hofmann, S. Imhof, M. Abdelghany, T. Kiessling, L. W. Molenkamp, C. H. Lee, A. Szameit, M. Greiter, and R. Thomale, arXiv preprint arXiv:1907.11562 (2019).
[89] C. H. Lee, L. Li, and J. Gong, Physical review letters **123**, 016805 (2019).
[90] S. Mu, C. H. Lee, L. Li, and J. Gong, arXiv preprint arXiv:1911.00023 (2019).
[91] See Supplementary Materials for details. (????).
[92] T. E. Lee, Physical review letters **116**, 133903 (2016).
[93] R. Resta, Ferroelectrics **136**, 51 (1992).
[94] C.-K. Chiu, J. C. Y. Teo, A. P. Schnyder, and S. Ryu, Reviews of Modern Physics **88**, 035005 (2016).
[95] D. Wang, S. Xu, Y. Wang, and C. Wu, Physical Review B **91**, 115118 (2015).
[96] L. Fidkowski, Physical review letters **104**, 130502 (2010).
[97] T. Grover, Physical review letters **111**, 130402 (2013).